

Metamaterial control of stimulated Brillouin scattering

M. J. A. Smith,^{1,2,*} B. T. Kuhlmeiy,¹ C. Martijn de Sterke,¹ C. Wolff,² M. Lapine,² and C. G. Poulton²

¹*Centre for Ultrahigh bandwidth Devices for Optical Systems (CUDOS) and Institute of Photonics and Optical Science (IPOS), School of Physics, The University of Sydney, NSW 2006, Australia*

²*Centre for Ultrahigh bandwidth Devices for Optical Systems (CUDOS),*

School of Mathematical and Physical Sciences, University of Technology Sydney, NSW 2007, Australia

(Dated: October 8, 2018)

Using full opto-acoustic numerical simulations, we demonstrate enhancement and suppression of the SBS gain in a metamaterial comprising a subwavelength cubic array of dielectric spheres suspended in a dielectric background material. We develop a general theoretical framework and present several numerical examples using technologically important materials. For As_2S_3 spheres in silicon, we achieve a gain enhancement of more than an order of magnitude compared to pure silicon, and for GaAs spheres in silicon, full suppression is obtained. The gain for As_2S_3 glass can also be strongly suppressed by embedding silica spheres. The constituent terms of the gain coefficient are shown to depend in a complex way on the filling fraction. We find that electrostriction is the dominant effect behind the control of SBS in bulk media.

Stimulated Brillouin scattering (SBS) is a nonlinear scattering process whereby an incident electromagnetic pump field coherently drives an acoustic wave through the material, scattering the pump field and inducing a frequency shift in the returning, or Stokes, field [1–4]. This scattering process features prominently in nonlinear optics, due to its relevance in the design of nanoscale devices such as on-chip tuneable photonic filters, Brillouin lasers and sensors [2]. That said, SBS is also regarded as a nuisance in optical communications systems, with considerable effort being focused on techniques for its suppression [5]. The usual process by which sound is coherently excited in the medium for SBS is electrostriction [6, 7], which describes when an electric field induces a strain field in the material. These strains can coherently drive a longitudinal acoustic wave through the medium, inducing a periodic variation in the optical properties of the material (via the photoelastic effect). It is the combination of electrostriction and photoelasticity which scatters the incident optical field [2, 5, 6]; thus, materials with strong photoelastic and electrostrictive properties also tend to exhibit strong SBS. Conversely, materials with weak electrostriction and photoelasticity are poor candidates for experimental demonstrations of SBS.

A recent theoretical study by the authors [8] demonstrated that the electrostrictive response of a material can be considerably enhanced or suppressed through the introduction of a subwavelength cubic array of spheres in a background material. Experimental work on doped silica fibres has also shown considerable promise [9]. Such results suggest that SBS is also affected through subwavelength structuring. This is the motivation behind our study into how metamaterial structuring influences the SBS response. In our work, we define an optoacoustic metamaterial as a structured material with period much smaller than both the acoustic and optical wavelengths in the material.

In this framework, we rigorously model the electrostrictive response of a metamaterial using perturbation procedures, with very few restrictive assumptions. The metamaterial we consider is a cubic array of spheres embedded in a background material. In contrast to existing work [8] which gave an analytical expression for the electrostriction within a hydrostatic approximation, we incorporate shear effects in our model (which are generally non-negligible in solid media but can easily be omitted for liquids). To evaluate the SBS gain, we also evaluate other photonic and acoustic parameters in the subwavelength limit, and incorporate the effects of acoustic loss. To the best of our knowledge, this is the first investigation on the SBS behaviour of metamaterials and we emphasise that the results presented are for intrinsic, or bulk, SBS properties. We theoretically obtain values for all parameters which feature in the SBS gain coefficient, all of which vary differently as we tune the filling fraction of our metamaterial and investigate different material combinations.

In addition to outlining a general theoretical framework, we present numerical results for a selection of silicon and chalcogenide glass-based metamaterials, to demonstrate suppression and enhancement of the intrinsic SBS gain coefficient. There is considerable interest in silicon-based materials due to a wide range of potential applications in the electronics industry, as silicon is CMOS-compatible [2]. That said, the biggest drawbacks in the use of conventional silicon as an SBS material are its inherently poor SBS gain coefficient, high speed of sound, and its large acoustic losses. We overcome these issues by introducing a suspension of spheres in the background material, and demonstrate an order of magnitude enhancement in the gain coefficient of bulk silicon using chalcogenide glass spheres. We also show absolute suppression of SBS in silicon using GaAs spheres.

The example we present for an As_2S_3 background material shows strong suppression in the SBS gain coefficient when structured with a cubic lattice of silica spheres, which means that SBS would be observed at much higher

* m.smith@physics.usyd.edu.au

TABLE I. **Bulk parameters at $\lambda_1 = 1550$ nm: refractive index n , photoelastic tensor coefficients p_{ij} , Brillouin frequency shift $\Omega_B/(2\pi)$ (units of [GHz]), Brillouin linewidth $\Gamma_B/(2\pi)$ (units of [MHz]), gain coefficient g_P (units of $[\text{m} \cdot \text{W}^{-1}]$), phonon viscosity coefficients η_{ij} (units of $[\text{mPa} \cdot \text{s}]$), stiffness tensor coefficients C_{ij} (units of [GPa]), material density ρ (units of $[\text{kg} \cdot \text{m}^{-3}]$), and acoustic velocity V_A (units of $[\text{m} \cdot \text{s}^{-1}]$) [10–16], where † are theoretical estimates, and subscripts are in Voigt form.**

Material	n	p_{11}	p_{12}	p_{44}	$\frac{\Omega_B}{2\pi}$	$\frac{\Gamma_B}{2\pi}$	$\max(g_P)$	η_{11}	η_{12}	η_{44}	C_{11}	C_{12}	C_{44}	ρ	V_A
Fused SiO ₂	1.45	0.12	0.27	-0.075	11.1	16	4.52×10^{-11}	1.6†	1.29†	0.16†	78.6	16.1	31.2	2200	5960
As ₂ S ₃	2.37	0.25	0.24	0.005	7.95	34	7.4×10^{-10}	1.8†	1.45†	0.18†	18.7	6.1	6.4	3200	2595
Si [100]	3.48	-0.094	0.017	-0.051	38†	320†	2.4×10^{-12} †	5.9	5.16	0.62	165.6	63.9	79.5	2329	8433
GaAs [100]	3.37	-0.165	-0.14	-0.072	21†	167†	2.0×10^{-10} †	7.49	6.57	0.72	119	53.4	59.6	5320	4734

laser powers (i.e. this increases the SBS threshold). Demonstrating SBS suppression in isotropic materials is relevant to those studying other nonlinear optical effects in common laser glasses, such as four-wave mixing, where undesired SBS effects can dominate.

The procedure for deriving the coupled intensity equations for electrostriction-induced SBS is well-known [3, 4, 17], and considers optical plane wave propagation in an isotropic bulk material. It gives rise to the SBS power gain spectrum

$$g_P = \frac{4\pi^2\gamma^2}{nc\lambda_1^2\rho V_A\Gamma_B} \left(\frac{(\Gamma_B/2)^2}{(\Omega_B - \Omega)^2 + (\Gamma_B/2)^2} \right), \quad (1)$$

where γ is a measure of the electrostrictive stress in the medium (defined precisely below), n is the refractive index, c is the speed of light in vacuum, λ_1 is the incident optical wavelength in vacuum, ρ is the mean material density, V_A is the longitudinal acoustic wave velocity, Ω is the angular frequency of the acoustic wave, $\Omega_B/(2\pi)$ denotes the Brillouin frequency shift, and Γ_B is the Brillouin line width at half maximum, with respect to angular frequency. Note that a conventional backwards SBS process has $\Omega_B = q_B V_A \approx 2\omega_1 n V_A / c$ where $\mathbf{q}_B = 2\mathbf{k}_1$ is the corresponding wave vector [3, 4] and ω_1 is the angular frequency of the incident optical field. The expression for γ is given in terms of the photoelastic tensor p_{ijkl} [18], which is defined in Einstein notation by

$$\Delta(\varepsilon_{ij}^{-1}) = p_{ijkl} s_{kl}, \quad (2)$$

where ε_{ij} is the relative permittivity tensor, $s_{ij} = \frac{1}{2}(\partial_i u_j + \partial_j u_i)$ is the strain tensor, u_i is the elastic displacement from equilibrium, and Δ denotes the change resulting from the strain. In this setting we have [5, 19]

$$\gamma = \gamma_{\text{xyyy}} = \varepsilon_{\text{r}}^2 p_{\text{xyyy}}. \quad (3)$$

Consequently, provided we obtain values for all terms in (1), then the gain coefficient can be determined and the SBS properties of a metamaterial are characterised. For reference, a range of material parameters [10–16] are shown in Table I.

We now proceed to obtain values for all terms in (1)–(3), beginning with an effective permittivity. Here, ‘effective’ refers to a long-wavelength description of the properties of a metamaterial as if it were a uniform material.

For reference, we specify the unit cell to be symmetric about the origin, defining d as the period of the cubic lattice, and a as the radius of the sphere, from which we define the filling fraction as $f = 4\pi a^3 / (3d^3)$. We remark that at dilute filling fractions the choice of lattice geometry is largely unimportant, although effects may be pronounced at higher filling fractions. The effective permittivity tensor is obtained here using a modification of the procedure outlined in [20], which is chosen for its conceptual simplicity and ease of numerical implementation (in this work, all problems are solved using a commercial finite element solver). This method involves first solving the eigenvalue problem for Maxwell’s equations for a number of Bloch vectors near the Γ point. For each vector we compute the volume averaged energy density [21]

$$U_{\text{avg}} = \frac{1}{2} \frac{1}{V_{\text{WSC}}} \varepsilon_0 \langle \varepsilon_{ij} E_i E_j^* \rangle, \quad (4)$$

where E_j is the electric field distribution of the Bloch mode, V_{WSC} is the volume of the Wigner-Seitz cell, and $\langle \rangle$ denotes volume integration over the cell. This quantity is then equated to the effective energy density expression

$$U_{\text{eff}} = \frac{1}{2} \frac{1}{(V_{\text{WSC}})^2} \varepsilon_0 \varepsilon_{ij}^{\text{eff}} \langle E_i \rangle \langle E_j \rangle^*, \quad (5)$$

giving rise to a linear system that is solved directly for the effective permittivity tensor. Following (3) we now determine the effective photoelastic constant $p_{\text{xyyy}}^{\text{eff}}$. This is obtained by mechanically perturbing the unit cell to approximate a strain induced by a longitudinal acoustic wave propagating through the metamaterial. Thus, we solve the acoustic wave equation [6] with zero body forces

$$-\rho \partial_t^2 u_i + \partial_j (C_{ijkl} \partial_k) u_l = 0, \quad \text{for } i = x, y, z, \quad (6)$$

inside the unit cell, assuming we are in the vicinity of Γ (i.e. we impose a time dependence of $\exp(-i\Omega t)$ where Ω is in the long wavelength limit) where C_{ijkl} denotes the stiffness tensor. To model the compression of the unit cell by the acoustic wave, we impose the boundary conditions

$$u_j \Big|_{\partial W_{\pm z}} = -Dz \delta_{zj} \Big|_{\partial W_{\pm z}}, \quad u_j n_j \Big|_{\partial W \setminus \{\partial W_{\pm z}\}} = 0, \quad (7)$$

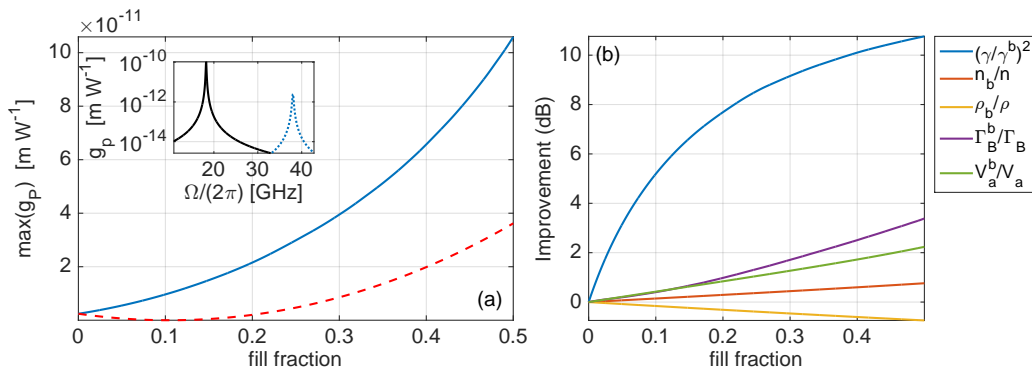


FIG. 1. (a) Gain coefficient for cubic lattice of As_2S_3 spheres in Si (blue) and GaAs spheres in Si (broken red) at $\lambda_1 = 1550$ nm for $d = 50$ nm, inset: gain coefficient for pure Si (dotted blue) and cubic lattice of As_2S_3 spheres in Si at $f = 50\%$ (black), (b) contribution from each term in (1) to improvement in g_p for As_2S_3 spheres in Si.

where ∂W denotes the boundary of the entire unit cell, D is the magnitude of the displacement, n_j are the components of the local normal vector to the surface, $\partial W_{\pm z}$ denote the faces of the cube with normal vectors $n_j = \pm \delta_{zj}$, and δ_{ij} is the Kronecker delta. This boundary condition generates a compressed unit cell geometry and an internal strain field which modifies the constituent permittivity tensors, making them spatially dependent (see (2)). Next, we repeat the procedure outlined in (4)–(5) to obtain an effective permittivity for the strained configuration, using the strained constituent permittivities. Having determined the strained and unstrained effective permittivity tensors (corresponding to an imposed strain over the unit cell of $s_{zz} = -D$), the $p_{\text{xxxy}}^{\text{eff}}$ coefficient for the metamaterial follows directly from the analogue to (2), after using the symmetry properties of cubic crystals [22].

To determine the remaining terms in (1) we examine the acoustic properties of the unstrained metamaterial and consider the acoustic wave equation (6) under the assumption of time-harmonic fields taken in the long wavelength limit. In this setting, the effective acoustic wave velocity is obtained by solving the acoustic eigenvalue problem and evaluating $V_A^{\text{eff}} = \tilde{\Omega}/\tilde{q}$, where $\tilde{\mathbf{q}} = 2\mathbf{k}_1 = (0, 0, 4\pi n_{\text{eff}}/\lambda_1)$ is the SBS resonant wave vector with corresponding acoustic frequency $\tilde{\Omega}$ and longitudinal mode \tilde{u}_j . We calculate the effects of acoustic loss using perturbation theory; we substitute $C_{ijkl} + \eta_{ijkl}\partial_t$ for C_{ijkl} in (6), where η_{ijkl} is the phonon dynamic viscosity tensor [6, 16]. Subsequently acoustic frequencies are perturbed as

$$\tilde{\Omega}^2 \rightarrow \tilde{\Omega}^2 + i\tilde{\Omega} \frac{\langle a_j \tilde{u}_j^* \rangle}{\langle \rho \tilde{u}_j \tilde{u}_j^* \rangle}, \quad (8)$$

where $a_i = \partial_j(\eta_{ijkl}\partial_k \tilde{u}_l)$. Numerically evaluating the square root of (8) one obtains $\tilde{\Omega} \rightarrow \tilde{\Omega}_R - i\tilde{\Omega}_I$ from which $\tilde{\Omega}_B = \tilde{\Omega}_R$ and $\tilde{\Gamma}_B = 2\tilde{\Omega}_I$ immediately follows [21]. We note that in order to evaluate the linewidth of a metamaterial one must possess the η_{ijkl} of the constituent materials, and these are generally not well-tabulated.

For uniform materials where η_{ijkl} are not available, estimates are obtained by using results from SBS experiments [11, 14] and imposing $u_j = \exp(iqz - i\Omega t)\delta_{zj}$ to obtain $\tilde{\Omega}^2 \rightarrow \tilde{\Omega}^2 - i\tilde{\Omega}q^2\eta_{zzzz}/\rho$. Taking the square root of both sides and evaluating a Taylor series in q ultimately gives

$$\eta_{zzzz} \approx \frac{V_A^2 \tilde{\Gamma}_B \rho}{\tilde{\Omega}_B^2}. \quad (9)$$

Following experimental data on η_{ijkl} [16] we estimate η_{yzyz} as being one order of magnitude smaller than η_{zzzz} , and assuming the material is isotropic, the identity $\eta_{yzyz} = \frac{1}{2}(\eta_{xxxx} - \eta_{xxyy})$ gives η_{xxyy} . Note that estimated values presented in Table I are denoted by †.

Having described the numerical procedures for determining all terms in (1) for the metamaterial, we now consider a selection of illustrative examples. For each choice of pairwise material combination, we consider the maximum gain coefficient (1) against the filling fraction (where the maximum filling fraction for a cubic lattice of spheres is $f = \pi/6 \approx 0.52$). We also consider how each parameter in (1) contributes to the gain coefficient by evaluating

$$10 \log_{10} \left(\frac{\max(g_p)}{\max(g_p^b)} \right) = 10 \log_{10} \left(\left(\frac{\gamma}{\gamma^b} \right)^2 + \dots \right),$$

and superposing a plot of all logarithmic terms in a single figure (where b denotes the background material). In this way, the contribution from each term is apparent because the improvement in the gain coefficient (in dB) is then the sum of each curve value at a given filling fraction. In Figure 1, we present the gain coefficient for a cubic lattice of As_2S_3 spheres in Si at $\lambda_1 = 1550$ nm, where the lattice period is $d = 50$ nm (solid blue curve). The period of the lattice is chosen to ensure that the structuring is both optically and acoustically subwavelength for all fill fractions: for the examples considered here, we have approximately 10 unit cells per optical wavelength. From Figure 1 we see that As_2S_3 spheres in Si gives an

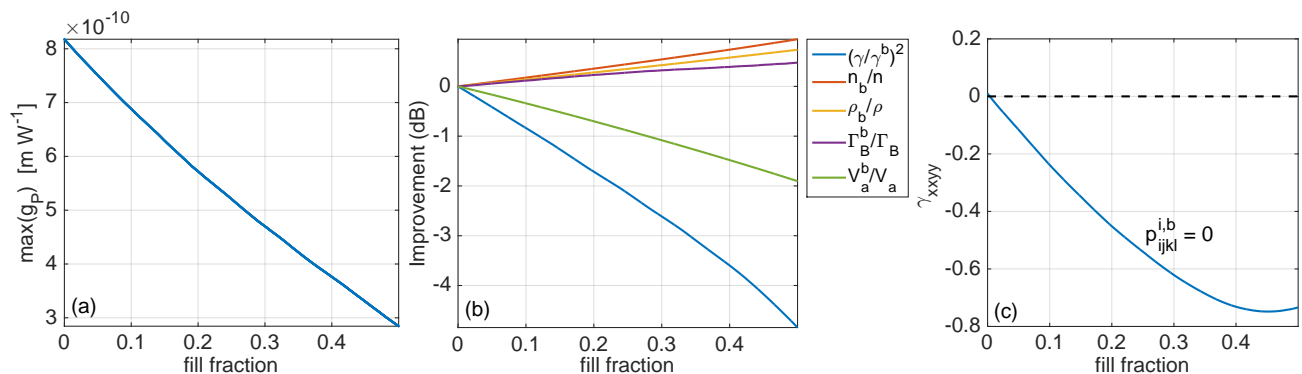


FIG. 2. (a) Gain coefficient for a cubic lattice of SiO_2 spheres in As_2S_3 at $\lambda_1 = 1550$ nm for $d = 50$ nm, (b) contribution from each term in (1) to improvement in g_P for SiO_2 spheres in As_2S_3 , (c) electrostriction parameter γ_{xxyy} for SiO_2 spheres in As_2S_3 when the inclusion and background material photoelastic tensors set to zero, showing a nonzero artificial contribution [8].

order of magnitude enhancement in the SBS gain ((1)) from the bulk Si value shown in Table I. In this case, an enhancement factor of more than 40 is achieved at $f = 50\%$ where $\max(g_P) = 1.06 \times 10^{-10} \text{ m} \cdot \text{W}^{-1}$, which is more than double that of pure fused SiO_2 (here we also have $\Gamma_B/(2\pi) = 147$ MHz and $\Omega_B/(2\pi) = 18$ GHz). The inset of Figure 1a shows the gain spectrum for silicon at $f = 0\%$ (dotted blue) and $f = 50\%$ (black) for the above example, where the enhancement and shift is visible. In Figure 1b, we observe that the SBS gain enhancement is largely driven by an increase in electrostriction, which is greater than the contributions from improvements in the refractive index, acoustic velocity, and Brillouin linewidth combined. Note that the increasing density of the metamaterial drives a decrease in the gain coefficient, but for this example, only slightly mitigates the improvements arising from the other parameters.

Also shown in Figure 1 is the gain coefficient for GaAs spheres in Si where complete suppression of SBS is achieved at a filling fraction of $f = 10\%$, and a $\max(g_P) = 3.6 \times 10^{-11} \text{ m} \cdot \text{W}^{-1}$ is achieved at $f = 50\%$. Note that at $f = 50\%$ we have structured Si with GaAs to obtain a gain coefficient comparable to pure fused SiO_2 , albeit with a broader linewidth of $\Gamma_B/(2\pi) = 223$ MHz and a greater frequency shift of $\Omega_B/(2\pi) = 27$ GHz. Analogously to the example with As_2S_3 spheres in Si, the SBS gain for GaAs spheres in Si for $f > 10\%$ is driven by enhancements in all parameters except for the effective material density (not shown). The $g_P = 0$ observed at $f = 10\%$ is caused by $p_{xxyy}^{\text{eff}} = 0$, which is in turn due to a sign change in constituent p_{xxyy} values (see Table I). In Figure 2a we show the gain coefficient for SiO_2 spheres in As_2S_3 , which demonstrates a more than 60% suppression in the gain coefficient at $f = 50\%$ (with corresponding values $\max(g_P) = 2.8 \times 10^{-10} \text{ m} \cdot \text{W}^{-1}$, $\Gamma_B/(2\pi) = 30$ MHz and $\Omega_B/(2\pi) = 9$ GHz). The explanation for this suppression is found in Figure 2b where reductions in the electrostriction and acoustic velocity outstrip positive contributions from all other remaining parameters. This points to the acoustic velocity playing an important

role in the suppression of SBS in metamaterials, in addition to the electrostriction. Note our calculated value for the SBS gain coefficient of As_2S_3 (i.e., at $f = 0\%$) is within 10% of the experimental value in Table I.

In Figure 2c we show γ_{xxyy} for the same configuration but when the photoelastic tensors of the constituent materials are set to zero. In spite of this, the metamaterial has a non-vanishing electrostriction parameter. This “artificial electrostriction” [8] arises from the different mechanical responses of the two constituent materials, and constitutes approximately 20% of the total γ_{xxyy} in Figure 2b at $f = 50\%$. The presence of artificial electrostriction demonstrates that the properties of the metamaterial cannot be understood through direct mixing, even when the structuring is subwavelength.

In summary, we have shown that both considerable enhancement and full suppression of SBS in silicon is achieved through a careful choice of inclusion material in a metamaterial comprising spheres in a cubic lattice. Calculations (not discussed here) on face-centred cubic lattices of spheres indicate that the specific lattice geometry has a minimal effect on the gain in the dilute limit. SBS is a complicated process, involving optical and acoustic waves together with their mutual interaction. We have implemented a rigorous microscopic procedure which encompasses all contributing physical processes.

The enhancement of the silicon gain coefficient to values greater than, or comparative to, fused silica is particularly promising for designers of small-scale, silicon based SBS devices. There is also considerable scope for metamaterials where the acoustic velocity contrast and the Brillouin linewidth contrast is high, as the contributions of these parameters have been shown here to play an important role in controlling SBS.

ACKNOWLEDGEMENTS

This work was supported by the Australian Research Council (CUDOS Centre of Excellence, CE110001018).

-
- [1] R. W. Boyd, K. Rzażewski, and P. Narum, Phys. Rev. A **42**, 5514 (1990).
- [2] B. J. Eggleton, C. G. Poulton, and R. Pant, Adv. Opt. Photonics **5**, 536 (2013).
- [3] P. E. Powers, *Fundamentals of nonlinear optics* (CRC Press, Boca Raton, 2011).
- [4] A. Kobaykov, M. Sauer, and D. Chowdhury, Adv. Opt. Photonics **2**, 1 (2010).
- [5] E. Peral and A. Yariv, IEEE J. Quantum Elect. **35**, 1185 (1999).
- [6] B. A. Auld, *Acoustic fields and waves in solids* (John Wiley & Sons, 1973).
- [7] C. Wolff, M. J. Steel, B. J. Eggleton, and C. G. Poulton, Phys. Rev. A **92**, 013836 (2015).
- [8] M. J. A. Smith, B. T. Kuhlmeier, C. M. de Sterke, C. Wolff, M. Lapine, and C. G. Poulton, Phys. Rev. B **91**, 214102 (2015).
- [9] P. Dragic, T. Hawkins, P. Foy, S. Morris, and J. Ballato, Nat. Photonics **6**, 627 (2012).
- [10] M. J. Weber, *Handbook of optical materials* (CRC press, Boca Raton, 2002).
- [11] K. S. Abedin, Opt. Expr. **13**, 10266 (2005).
- [12] J. M. Rouvaen, E. Bridoux, M. Moriamez, and R. Torguet, App. Phys. Lett. **25**, 97 (1974).
- [13] R. K. Galkiewicz and J. Tauc, Solid State Commun. **10**, 1261 (1972).
- [14] R. Pant, C. G. Poulton, D. Y. Choi, H. Mcfarlane, S. Hile, E. Li, L. Thevenaz, B. Luther-Davies, S. J. Madden, and B. J. Eggleton, Opt. Expr. **19**, 8285 (2011).
- [15] D. K. Biegelsen, Phys. Rev. Lett. **32**, 1196 (1974).
- [16] B. G. Helme and P. J. King, Phys. Status Solidi A. **45**, K33 (1978).
- [17] G. P. Agrawal, *Nonlinear fiber optics*, 2nd ed. (Academic press, San Diego, 1995).
- [18] R. E. Newnham, *Properties of Materials: Anisotropy, Symmetry, Structure: Anisotropy, Symmetry, Structure* (Oxford University Press, New York, 2004).
- [19] P. T. Rakich, P. Davids, and Z. Wang, Opt. Expr. **18**, 14439 (2010).
- [20] D. J. Bergman, Phys. Rep. **43**, 377 (1978).
- [21] J. D. Jackson, *Classical Electrodynamics*, 2nd ed. (Wiley, New York, 1962).
- [22] J. F. Nye, *Physical properties of crystals: their representation by tensors and matrices* (Oxford university press, Suffolk, 1985).